DOI: 10.26599/FSHW.2025.9250841

Contents lists available at SciOpen

Food Science and Human Wellness

journal homepage: https://www.sciopen.com/journal/2097-0765

China Food Publishing Co.

Protective effects of *Ficus hirta* Vahl. intestinal epithelial cells injury through the microRNA-195/HNMT pathway *in vitro* and *in vivo*

Yingjie Wang[a], Yuhan Chen[a], Wen Dang[a], Xueni Zhang[a], Mengli Qing[a], Huiming Hua[a], Di Zhou[a,*], Gang Chen[a,b,*], Ning Li[a,*]

[a] *School of Traditional Chinese Materia Medica, Key Laboratory of Innovative Traditional Chinese Medicine for Major Chronic Diseases of Liaoning province, Key Laboratory for TCM Material Basis Study and Innovative Drug Development of Shenyang City, Shenyang Pharmaceutical University, Shenyang 110016, P.R. China.*

[b] *Research Center for High Altitude Medicine, Key Laboratory for High Altitude Medicine (Ministry of Education), Laboratory for High Altitude Medicine of Qinghai Province, Qinghai University, Xining 810001, China.*

ABSTRACT: This study elucidates the intestinal epithelial protective effects of EFhV, the ethanol extract of *Ficus hirta* Vahl, a popular edible plant. *In vitro* experiments demonstrated that EFhV enhances proliferation/migration of IEC-6 and HCoEpiC cells, reverses drug-induced growth inhibition (e.g., DFMO, clindamycin hydrochloride), and alleviates cell cycle arrest (G0/G1 phase). Mechanistically, EFhV downregulates microRNA-195, which targets histamine *N*-methyltransferase (HNMT), thereby restoring HNMT expression at both mRNA and protein levels. *In vivo* experiments confirmed EFhV's efficacy in mitigating intestinal epithelial damage in fasting and antibiotic rat models, normalizing miR-195/HNMT dysregulation. These findings reveal the miR-195/HNMT axis as a key pathway through which EFhV promotes intestinal repair and homeostasis, supporting its potential as a dietary intervention for gut barrier protection and digestive disorder management.

Key words: *Ficus hirta* Vahl.; Intestinal epithelium; microRNA-195; Histamine N-methyltransferase;

1. Introduction

The intestine serves as a vital organ for digestion and immunity, playing a crucial role in maintaining overall physiological functions and preventing disease. The stabilization of intestinal epithelial homeostasis relies on the mucosal barrier formed by intestinal epithelial cells[1]. This barrier selectively facilitates the permeation of water and small molecule nutrients while preventing the entry of macromolecules, including bacteria. The intestine maintains dynamic equilibrium in intestinal epithelial homeostasis through the self-renewal of the intestinal epithelium, balancing the proliferation and apoptosis of intestinal epithelial cells, and repairing damage[2-4]. However, prolonged exposure to exogenous microorganisms, toxins, and metabolic stress can disrupt intestinal homeostasis due to factors such as antibiotic overuse, nutritional imbalance, and inflammation[5,6]. Antibiotics not only disturb gut microbiota balance but also compromise

***Corresponding author**
zhoudi930322@163.com (D. Zhou);
chengang1152001@163.com (G. Chen);
liningsypharm@163.com (N. Li).

Received 17 June 2025
Received in revised from 17 July 2025
Accepted 31 July 2025

mucosal barrier function, increase intestinal permeability, and exacerbate inflammation[7,8]. Hunger or nutritional deficiency further amplifies the risk of intestinal damage by inducing epithelial cell apoptosis, microbiota dysbiosis, and immune dysfunction[9]. Research into intestinal barrier repair and microbiota regulation has garnered significant attention. Bioactive compounds derived from natural food sources, interact synergistically with the intestinal ecosystem to preserve barrier integrity and homeostatic equilibrium through multi-target modulation of gut microbiota composition, anti-inflammatory signaling pathways, and epithelial tight junction protein expression[10-12].

Ficus hirta Vahl., also known as "*hairy Fig*" or "*Radix Fici Hirtae*", a plant belonging to the genus *Ficus* within the Moraceae family. It is predominantly cultivated in southern regions of China, including Guangdong and Yunnan provinces. It is colloquially referred to as "Southern Astragalus" or "Cantonese Ginseng," and is highly valued for its distinctive coconut-milk-like aroma and health-enhancing properties. Widely employed in Lingnan cuisine, its roots play a crucial role in the preparation of soups, herbal remedies, and teas. Over 80% of households in southern China regularly incorporate it into their seasonal broths, such as "*hairy fig-pork spine bon*e soup", "*hairy fig-chicken soup*", etc. The roots of *F. hirta* are used in Lingnan folk medicine to strengthen the spleen, resolve dampness, tonify qi, and consolidate the exterior, and are employed to treat digestive ailments including anorexia, indigestion, and dyspepsia[13]. Contemporary research further elucidates its rich content of active compounds, including phenylpropanoids, flavonoids, and polysaccharides[14-16], which confer multiple pharmacological effects, such as antioxidation, anti-inflammation, immune regulation, hepatoprotection, intestinal protection, and anti-tumor activity[17,18]. Although *F. hirta* has exhibited therapeutic potential in enhancing gastrointestinal tract function and promoting digestive system health[13], its protective effects against intestinal epithelial cell injury remain unexplored. Here we evaluated the effect of ethanol extract of *F. hirta* Vahl. (EFhV) on promoting the growth of intestinal epithelial cells, and its post-transcriptional mechanism was further systematically investigated.

Post-transcriptional gene regulation plays a key role in the development of many diseases, including intestinal and lung epithelial injuries. MicroRNA-195, as a member of the miR-15/107 family, may play a critical role in the pathogenesis of various diseases due to its dysregulation[19]. For example, studies have demonstrated that the upregulation of miR-195 promotes apoptosis in hepatoma cells by enhancing the expression of LATS2 and P53 while simultaneously reducing the expression of cyclin-dependent kinase 2 (CDK2)[20]. miR-195 regulates intestinal epithelial restitution after wounding by altering actin-related protein-2 translation[21]. Additionally, miR-195 suppresses the proliferation, migration, invasion, and epithelial-mesenchymal transition (EMT) processes of gastric adenocarcinoma cells by targeting OTX1, thereby reducing its expression and promoting cell apoptosis[22]. In our previous study[23], we discovered that abnormal expression of microRNA-195 could inhibit the migration of intestinal epithelial cells, compromise the integrity of the intestinal epithelium, and impair the intestinal epithelial barrier function. To date, no studies have reported on the mechanism by which natural drug extracts regulate microRNA-195 to exert

protective effects on intestinal epithelial cells. Meanwhile, histone N-methyltransferase (HNMT), as a biomarker indicative of intestinal mucosal integrity, exhibits differential expression in intestinal diseases[24,25]. However, the underlying functional mechanisms of HNMT remain to be fully elucidated.

This study innovatively reveals for the first time, from the perspective of post-transcriptional regulation, that the EFhV exerts protective effects on the intestinal epithelium *in vivo* and *in vitro* through the miR-195/HNMT signaling axis, thereby demonstrating the potential medicinal value of *F. hirta*. Furthermore, this study lays a theoretical foundation for the subsequent development of intestinal protective preparations.

2. Materials and methods

2.1 Animals and Experiment

All procedures followed the People's Republic of China Research Council's Guide for the Care and Use of Laboratory Animals. SPF SD rats (male and female, 200-230 g, certificate: SYPU-IACUC-S2022-11.24-201) were purchased from GemPharmatech Co., Ltd., they were randomly assigned to the control group, the Antibiotic or Fasting model group, and the treatment groups (positive drug group, EFhV low-dose group, EFhV high-dose group), with eight rats in each group. Each rat was individually identified by numbering on its tail. The health status of the rats was monitored daily, and their body weights were recorded systematically.

In the fasting model, the experiment was conducted over a period of 4 days. Rats in the control group were fed freely throughout the experiment, while rats in the model group were fed normally for the first 48 h and subsequently subjected to water-free fasting for the following 48 h. Rats in the treatment group received daily intragastric administration of Glycyrrhetinic acid (25 mg/kg) and the EFhV (250 mg/kg and 750 mg/kg) during the initial 48 h period. The control and model groups received an equivalent volume of CMC-Na via intragastric administration during this time. During the subsequent 48 h fasting period, medication was administered as scheduled. On the fifth day, the rats were euthanized, and tissue samples were collected. In the antibiotic model, the experiment was conducted over a period of 14 days. The (Clindamycin HCl, 250 mg/kg) were administered daily by intragastric administration, except for the control group. After one week, the administration group was intragastric administration GA (25 mg/kg) and EFhV (250 mg/kg, 750 mg/kg) at the same time daily for 7 consecutive days. The control group and the model group received the same volume of CMC-Na. The rats were euthanized at fifteenth day, and their tissue were collected.

2.2 Cell Culture

The rat intestinal epithelial cells (IEC-6) were obtained from the Kunming Cell Bank of the Chinese Academy of Sciences (Kunming, China), while human colon epithelial cells (HCoEpiC) were acquired from Shenzhen Haodi Huatuo Biological Co., Ltd (Shenzhen, China). And the cryopreserved cells were rapidly thawed in a 37℃ water bath, centrifuged at 1800 r/min for 5 min, and resuspended in complete medium. IEC-6 and HCoEpiC cells were cultured in DMEM (Biological Industries, Israel) supplemented with 10%

fetal bovine serum (FBS; Bioind, Israel), all with 1% penicillin/streptomycin. Cells were incubated at 37℃ under 5% CO_2, and the medium was replaced within 24 h. For subculture, cells were passaged at ~90% confluence by rinsing with PBS, digesting with 0.25% trypsin-EDTA (IEC-6: ~2.5 min, HCoEpiC: 7-8 min; Bioind, Israel), and they were reseeded at split ratios of 1 : 3. For cryopreservation, cells were detached, centrifuged, resuspended in freezing medium (culture medium : DMSO = 19:1), transferred to cryovials, stored at -80℃ overnight, and finally preserved in liquid nitrogen. All experiments were conducted using cells passaged ≤3 times.

2.3 Cell Cycle and Apoptosis

Cells were plated in 6-well plates and cultured 48 h under standard conditions, consistent with our earlier viability assays. After trypsin digestion, the cells were gently resuspended by pipetting, and the resulting cell suspension was transferred to an EP tube. Then centrifuged at 7500 r/min for 5 minutes at 4℃. Following centrifugation, the supernatant was discarded, and the cell pellet was washed once with 1 mL of pre-cooled PBS and re-centrifuged under the same conditions. Subsequently, 1 mL of lysis buffer and 10 μL of DNA staining solution were added to each sample. The samples were incubated at room temperature in the dark for 30 minutes.

Flow cytometry analysis was performed within 1 hour after filtering the samples, and the results were analyzed using ModFit software. For apoptosis detection, identical culture conditions were applied. Harvested cell suspensions were co-stained with FITC-labeled Annexin V and PI (Wanleibio, China) for 15 min at room temperature in the dark. All samples were analyzed using a BD FACSVerse flow cytometer. Data processing software calculated the percentage of cells in each cell cycle phase (G0/G1, S, G2/M) and quantified early/late apoptotic populations.

2.4 Measurement of Cell Viability (MTT assay)

Cell viability was measured with MTT assays. IEC-6 and HCoEpiC Cells were cultured in 96-well plates (100 μL/well) at appropriate densities and incubated for 12 h. Model groups were treated with 5 mmol/L DFMO, 300 μmol/L clindamycin hydrochloride, or miR-195-3p mimics, while the treatment groups received EFhV at concentrations of 5, 10, 20, 50, or 100 μg/mL. Control wells were supplemented with an equal volume of fresh medium. All groups included at least triplicate wells and were cultured under 5% CO_2 at 37℃ for 48 or 96 h. Then, 50 μL of MTT solution (2 mg/mL in PBS) was added to each well without medium removal. After 4 h of incubation in the dark, supernatants were discarded, and 100 μL DMSO was added to dissolve formazan crystals. The plates were shaken at 250 r/min for 5 min, and optical density (OD) at 490 nm was measured using a microplate reader (Thermo Fisher Scientific, USA).

2.5 Plant Material

The the roots of *Ficus hirta* Vahl were purchased from Songchuntang Pharmacy (Foshan Nanhai District) Co., Ltd., and authenticated by Professor Li Yanwu from the Traditional Chinese Medicine University of Guangzhou.

2.6 Hoechst 33258 Staining

Hoechst 33258 staining reagent was used to observe the morphological changes of apoptotic cells. Upon binding to double-stranded DNA, cell nuclei were stained blue. Subsequently, cell apoptosis was quantitatively analyzed by flow cytometry. Cells were evenly distributed in a 6-well plate and treated with the samples for 48 h, the culture medium was aspirated, and cells were fixed with 0.5 mL of 4% paraformaldehyde solution for 30 min. After fixation, paraformaldehyde was aspirated, and cells were washed twice with 1 mL of PBS on a shaker for 3 min each time. Hoechst 33258 staining solution (0.5 mL per well) was added, and staining proceeded in the dark for 1 h. Following staining, the Hoechst 33258 solution was removed, and cells were washed twice with PBS. The samples were then sealed and imaged under a fluorescence microscope.

2.7 H&E Staining

The small intestine and colon tissue samples of rats were cut into pieces, fixed in 4% paraformaldehyde, paraffin-embedded, and sectioned for pathologically analysis.

2.8 Immunochemistry Assay

Antigen retrieval was performed using citrate buffer (pH 6.0) at 100℃ for 5-8 min, allowing the buffer to cool naturally to room temperature, and repeat twice and finally wash with PBS for 5 min. Then, add a 3% H_2O_2 solution to the sections, incubate at room temperature for 10 min, wash with PBS for 5 min, and repeat this process three times. Non-specific binding sites were blocked with 1% bovine serum albumin (BSA; Sigma-Aldrich) in PBS for 30 min at 4℃. Then, primary antibody incubation was performed overnight at 4℃, and remove the primary antibody and wash with PBS three times for 10 min each. Subsequently, add the secondary antibody dropwise and incubate at room temperature for 30 min. After removing the secondary antibody, wash with PBS three times for 10 min each. Add the freshly prepared DAB solution dropwise, and incubate in a humidified chamber. Monitor the staining intensity under a microscope. Following staining, wash the sections three times with PBS for 5 min each. Restain with hematoxylin for 5 min and rinse thoroughly with distilled water. Subsequently, immerse the slices in a 1% hydrochloric acid-alcohol solution for 3-5 s, followed by rinsing with distilled water. Finally, restore the blue coloration in PBS. Images were acquired via laser-conflicted microscopies (Olympus, Japan) after staining.

2.9 RT-qPCR Analysis

As recommended by the manufacturer, total RNA was isolated from cells using Trizol reagent (TaKaRa, China). The RNA concentration and purity were examined by an Eppendorf unit, and cDNA was generated through a reverse transcription kit (Sangon Biotech, China). Subsequently, the Mx3000P system (Bio-Rad, USA) was utilized to perform Quantitative real-time PCR with SYBR Premix EXtag II (TaKaRa, China). The relative expression levels were calculated using the same method as previously reported[26], and all samples were analyzed three times to verify the results.

2.10 Western Blot Analysis

Proteins from cells or guts were extracted with lysis solution, and the specific steps were the same as in previous methods[23]. Briefly, proteins were transferred to methanol-activated PVDF membranes (70 V, 90 min, ice-cooled) and blocked with 5% skim milk in TBST. Membranes were incubated with primary antibodies (4℃ overnight) and HRP-conjugated secondary antibodies (room temperature, 1.5 h), followed by TBST washes. ECL substrate was applied, and bands were visualized using a gel imaging system. Quantification was performed with Gelpro32 software.

2.11 Wound Healing Assay

The IEC-6 and HCoEpiC cells in the Tissue Culture Dishes (60 mm) were sown and cultivated under 37℃ and 5% CO until they were completely grown. For IEC-6 cells, a straight wound was created by scraping cells along a pre-marked line (0.5 cm intervals) using a coverslip, while HCoEpiC cells were scratched centrally with a 1 mL pipette tip to ensure uniform linear wounds. After PBS washing to remove debris, cells were treated with medium, drugs (blank, treatment, or transfected groups), or controls. Initial images (0 h) of the wound area were captured using an inverted microscope, followed by incubation under standard conditions. The same marked regions were re-imaged at 24, 48, 72, and 96 h. Image J was applied to manipulate the scratch images.

2.12 Statistical Analysis

The experimental data was represented in the form of mean ± SEM. Unpaired t tests and one-way ANOVA were utilized to detect the considerable disparities between specific groups, with a $P < 0.05$ considered as statistically significant. All data was processed through GraphPad Prism 9.

3. Results and discussion

3.1 The EFhV promotes proliferation in IEC-6 and HCoEpiC cells

The roots of *Ficus hirta* Vahl were subjected to extraction with 95% ethanol to yield the ethanol extract (EFhV, Figure 1A). First, MTT method was used to assess the effect of EFhV rat intestinal epithelial cell (IEC-6) growth. The results showed that EFhV could promote ICE-6 cell growth in a dose-dependent manner (20-100 μg/mL, Figure 1B). Therefore, the effective dose of EFhV (20, 50, 100 μg/mL) was used to conduct the following experiments. Flow cytometry results indicated that EFhV (20, 50 μg/mL) significantly promoted ICE-6 cells proliferation by increasing the proportion of S phase, and changing the distribution of G2/M phase (Figure 1C). However, after 48 h of treatment with EFhV (20, 50 μg/mL), there was no significant impact on cell apoptosis compared to the control group (Figure 1D). Additionally, an experiment was carried out to evaluate the restitution after wounding of IEC-6 cells. Following cellular injury, the administration of the highest effective dose of EFhV (50 μg/mL) significantly enhanced cellular migration (Figure 1E). This promoting effect became increasingly pronounced over time, indicating that EFhV plays a crucial role in facilitating the repair process of IEC-6 cells.

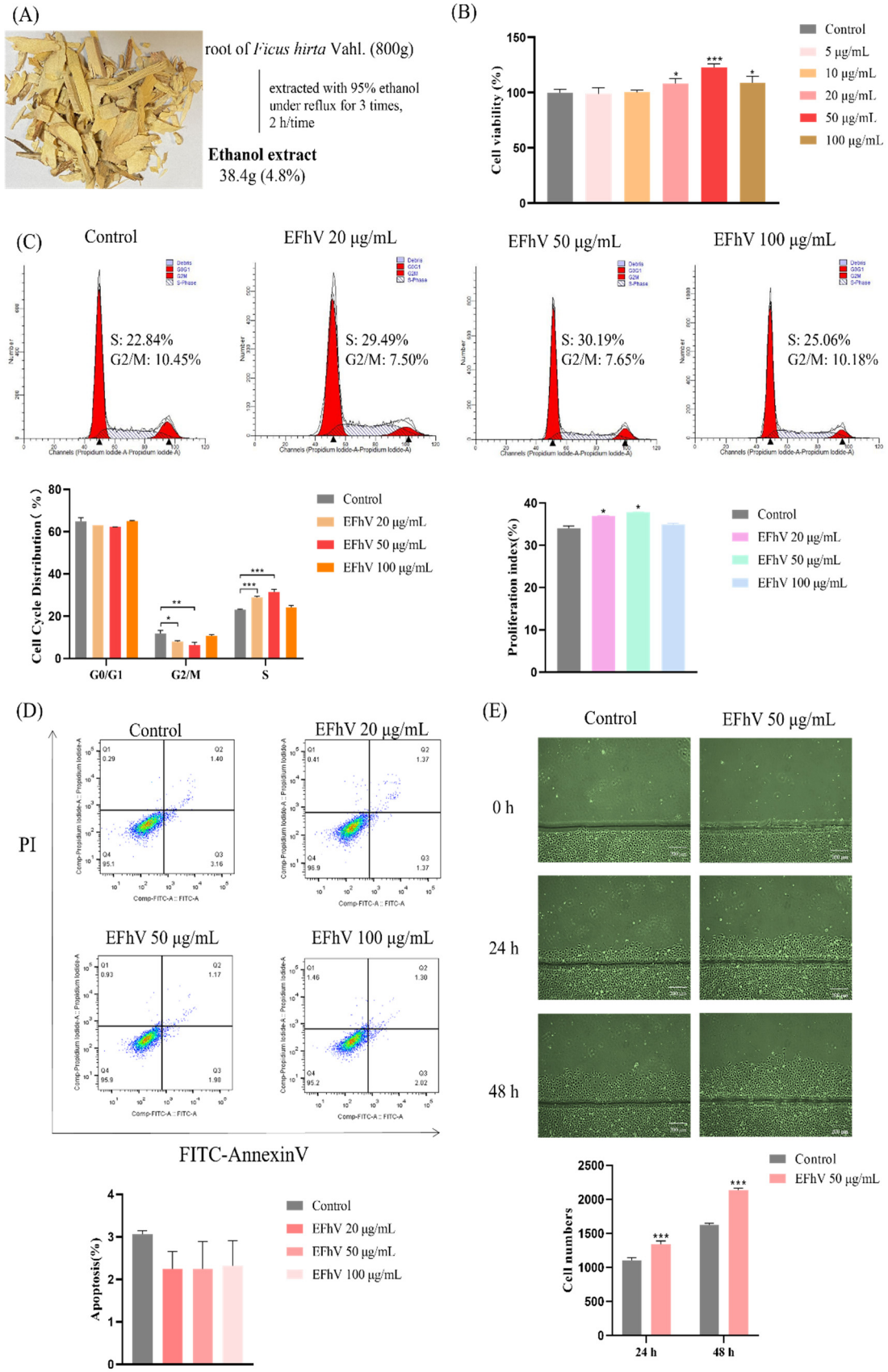

Figure 1. Effects of EFhV on the activity of IEC-6 cells. (A) The process of ethanol extract of the roots of *Ficus hirta* Vahl. (B) Effects of ethanol extract of *Ficus hirta* Vahl. (EFhV) on IEC-6 cells viability. (C-D) Effects of EFhV on cell cycle and apoptosis of IEC-6 cell. (C) The cell cycle of IEC-6 cell treated with EFhV was measured by flow cytometry. (D) The apoptosis of IEC-6 cell treated with EFhV was detected by flow cytometry. (E) Effect of EFhV on IEC-6 cell migration. Statistical significance was assessed by one-way ANOVA. Values are means ± SEM, n = 3. *$P < 0.05$, **$P < 0.01$, ***$P < 0.001$ compared with the control group.

Building on the observed proliferative effects of EFhV on IEC-6 cells, this study further investigated its species-specific impacts on intestinal homeostasis by extending the analysis to human colonic epithelial cells (HCoEpiC). This dual-model approach systematically evaluates EFhV's regulatory functions across distinct species and anatomically separate intestinal segments (proximal small intestine *vs.* distal large intestine).

Specifically, HCoEpiC cells were exposed to varying concentrations of EFhV for 48 hours. As a result, EFhV at concentrations of 50 μg/mL and 100 μg/mL significantly promoted proliferation in HCoEpiC cells (Figure 2A). Flow cytometry analysis revealed that EFhV may exert its proliferative effects by targeting the S phase of the cell cycle in HCoEpiC (Figure 2B). However, after 48 h of EFhV treatment, no significant effect on cell apoptosis was observed in either HCoEpiC cells compared to the control group (Figure 2C). Furthermore, an experiment evaluating the restitution after wounding of HCoEpiC cells was performed. Following induced cell injury, the application of EFhV significantly enhanced cellular migration (Figure 2D), indicating that EFhV also can promote the repair process in HCoEpiC cells.

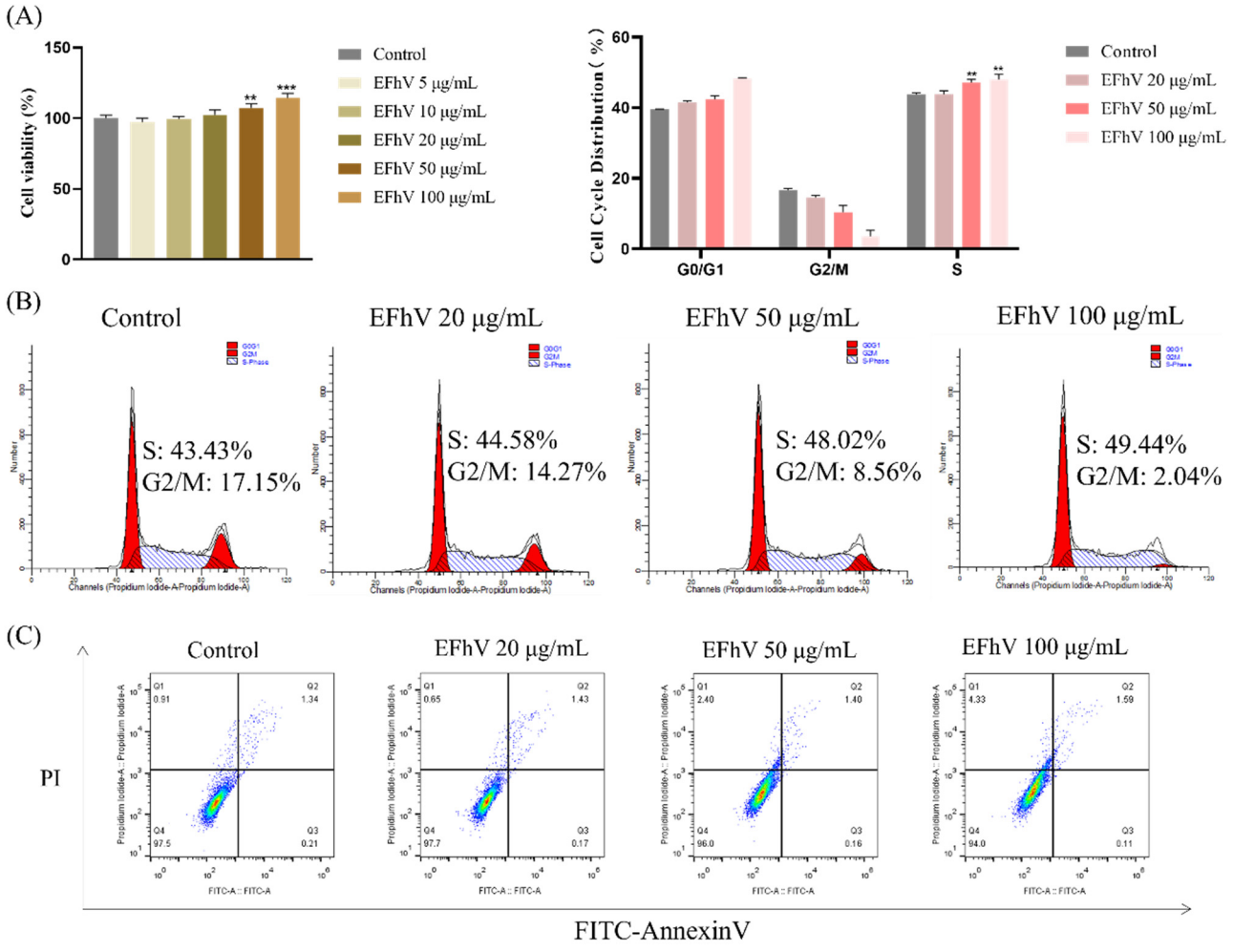

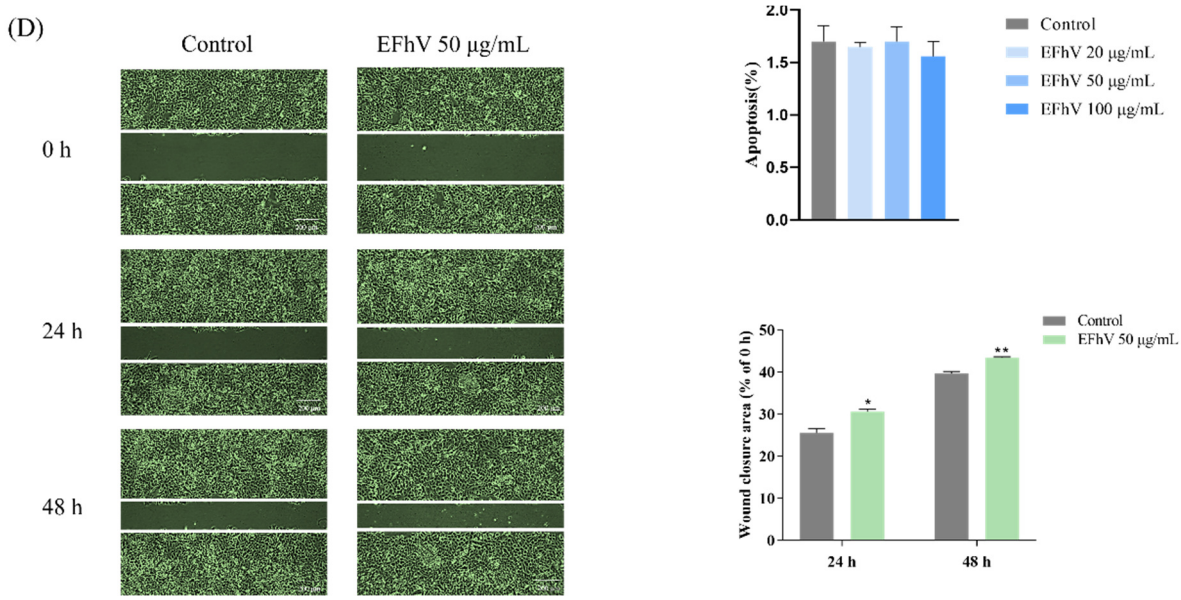

Figure 2. Effects of EFhV on the activity of HCoEpiC cells. (A) Cell viability of HCoEpiC treated with EFhV. (B) The cell cycle of HCoEpiC was measured by flow cytometry. (C) The apoptosis of HCoEpiC was detected by flow cytometry. (D) Cell migration experiment of HCoEpiC cells treated with EFhV 50 μg/mL. Values are means ± SEM, n = 3. **P* < 0.05, ***P* < 0.01, ****P* < 0.001 compared with the control group.

3.2 EFhV reverses the damage on IEC-6 and HCoEpiC cells induced by DFMO

Difluoromethylornithine (DFMO) serves as an irreversible inhibitor of ornithine decarboxylase (ODC). It exerts growth-inhibitory effects on intestinal epithelial cells and compromises the integrity of the intestinal mucosa by reducing intracellular polyamine levels[23]. Here, we employed two DFMO-induced intestinal epithelial cell damage models, including IEC-6, and HCoEpiC cells, to investigate the effects of EFhV on the growth inhibition of intestinal epithelial cells (Figure 3). The MTT assay results showed that IEC-6 cell growth was significantly inhibited after 48 h and 96 h of DFMO (5 mmol/L) treatment, with a marked significantly decrease in survival rate compared to the control group. After treatment (50 μg/mL) for 48 h and 96 h reversed the growth inhibition of IEC-6 cells (Figure 3A). Furthermore, wound-healing experiment were conducted to evaluate the effects of EFhV on the migration of IEC-6 cells in the DFMO-induced model, as shown in Figure 3B. The results demonstrated that the number of IEC-6 cells migrating into the scratch area was significantly reduced after DFMO treatment at 24 h, 48 h, 72 h, and 96 h compared to the untreated control group. However, treatment with the EFhV 50 μg/mL for 96 h significantly restored the migratory capacity of HCoEpiC cells in the DFMO-induced model. In addition, wound-healing assay (Figures 3C-3D) indicated that HCoEpiC cells also exhibited significantly reduced migration following DFMO treatment at 24 h, 48 h, 72 h, and 96 h, while EFhV (50 μg/mL) markedly reversed the inhibition of cell growth and impaired cell repair induced by DFMO.

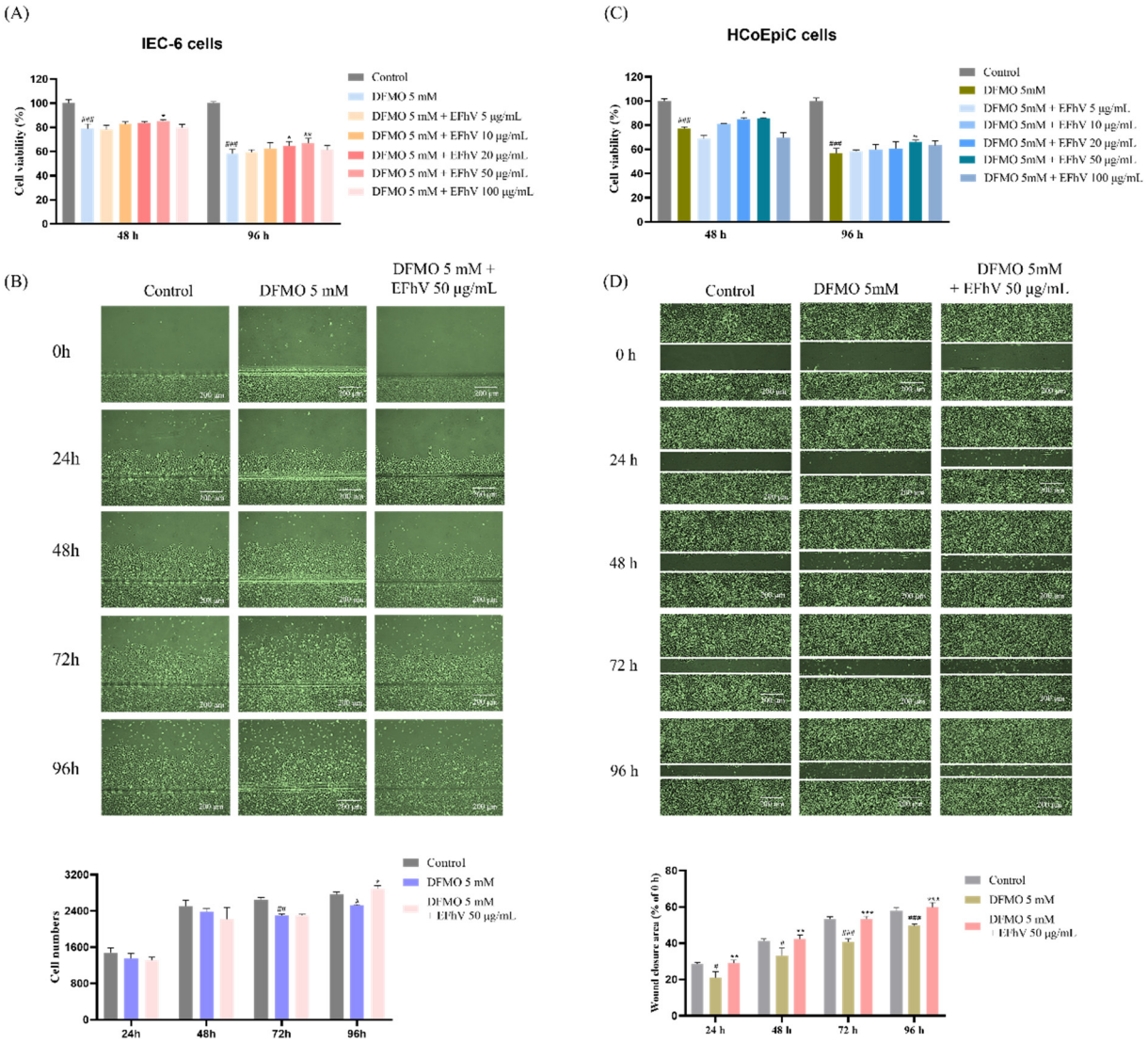

Figure 3. Effects of EFhV on IEC-6 and HCoEpiC cells damage induced by DFMO. (A) The cell viability of IEC-6 cells treated with DFMO (5 mmol/L) and EFhV at different concentrations. (B) Effects of DFMO and EFhV 50 μg/mL on IEC-6 cell migration.(C) The cell viability of HCoEpiC cell treated with DFMO (5 mmol/L) and EFhV at different concentrations. (D) Effects of DFMO and EFhV 50 μg/mL on HCoEpiC cell migration. Values are means ± SEM, n = 3. $^{*}P < 0.05$, $^{**}P < 0.01$, $^{***}P < 0.001$ compared with the control group. $^{\#}P < 0.05$, $^{\#\#}P < 0.01$, $^{\#\#\#}P < 0.001$ compared with control group and $^{*}P < 0.05$, $^{**}P < 0.01$, $^{***}P < 0.001$ compared with DFMO group.

3.3 EFhV reverses the damage on IEC-6 cells, and HCoEpiC cells induced by antibiotic

Excessive antibiotics and prolonged exposure can destroy physiological functions, induce structural changes in the body, mostly adverse reactions, and may even lead to secondary infections. Studies have demonstrated that antibiotics can induce intestinal epithelial and colon damage, impair barrier function, and potentially trigger chronic intestinal inflammation in forindividuals predisposed to inflammation[27,28]. Clindamycin Hydrochloride (Clindamycin HCl), a commonly used antibiotic, may cause gastrointestinal adverse reactions such as diarrhea and pseudomembranous colitis, and is frequently employed to induce intestinal barrier dysfunction in experimental models[26]. In this study, the Clindamycin-induced IEC-6 and HCoEpiC cell models were utilized to assess the inhibitory effect of EFhV on cell growth, as well as its ability to repair injury. The MTT assay results demonstrated that EFhV at a concentration of 50 μg/mL was most effective in reversing the growth inhibition of both IEC-6 and HCoEpiC cells (Figures 4A-4B).

Consequently, of EFhV (50 μg/mL) was employed in subsequent experiments. Wound-healing assay indicated that concurrent administration of EFhV could significantly enhance the post-injury repair of IEC-6 cells and HCoEpiC cells compared to the model group (Figure 4C-4D). The cell proliferation marker Ki67 in the IEC-6 cell antibiotic model was evaluated using a cellular immunofluorescence assay, with results shown in Figure 4E. Following treatment with antibiotics for 48 h, Ki67 expression in IEC-6 cells was significantly reduced. Administration of EFhV to IEC-6 cells for 48 h resulted in increased Ki67 expression and accelerated cell proliferation compared to the model group. Furthermore, the influence of EFhV on the cell cycle was confirmed through PI monostaining and flow cytometry analysis (Figure 4F). After 48 hours of antibiotic exposure, the cell cycle of IEC-6 cells was arrested in the G0/G1 phase, leading to significant growth inhibition. Treatment with EFhV (50 μg/mL) effectively alleviated the G0/G1 phase arrest induced by antibiotics. These findings indicate that EFhV (50 μg/mL) can significantly reverse the inhibitory effects of antibiotics on cell growth. Hoechst 33258 staining was employed to visualize cell nuclei (Figure 4G). Under an inverted fluorescence microscope, uniform nuclear staining was observed in the blank control group, with no evident signs of apoptosis. And no significant apoptosis was detected in either the antibiotic-treated group or the combination treatment group. Similarly, EFhV (50 μg/mL) effectively alleviated the G0/G1 phase arrest in the antibiotic-induced HCoEpiC cells model (Figure 4H).

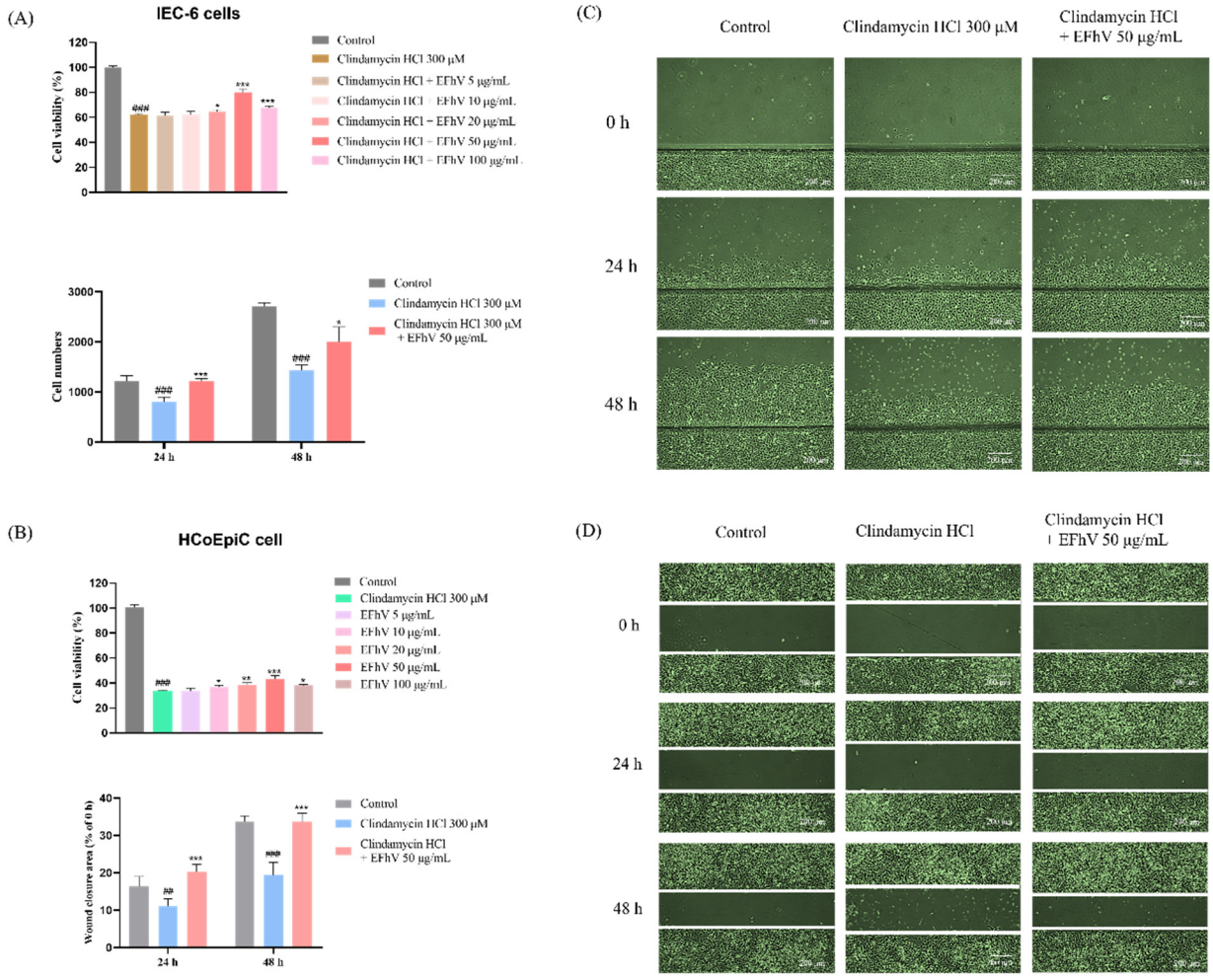

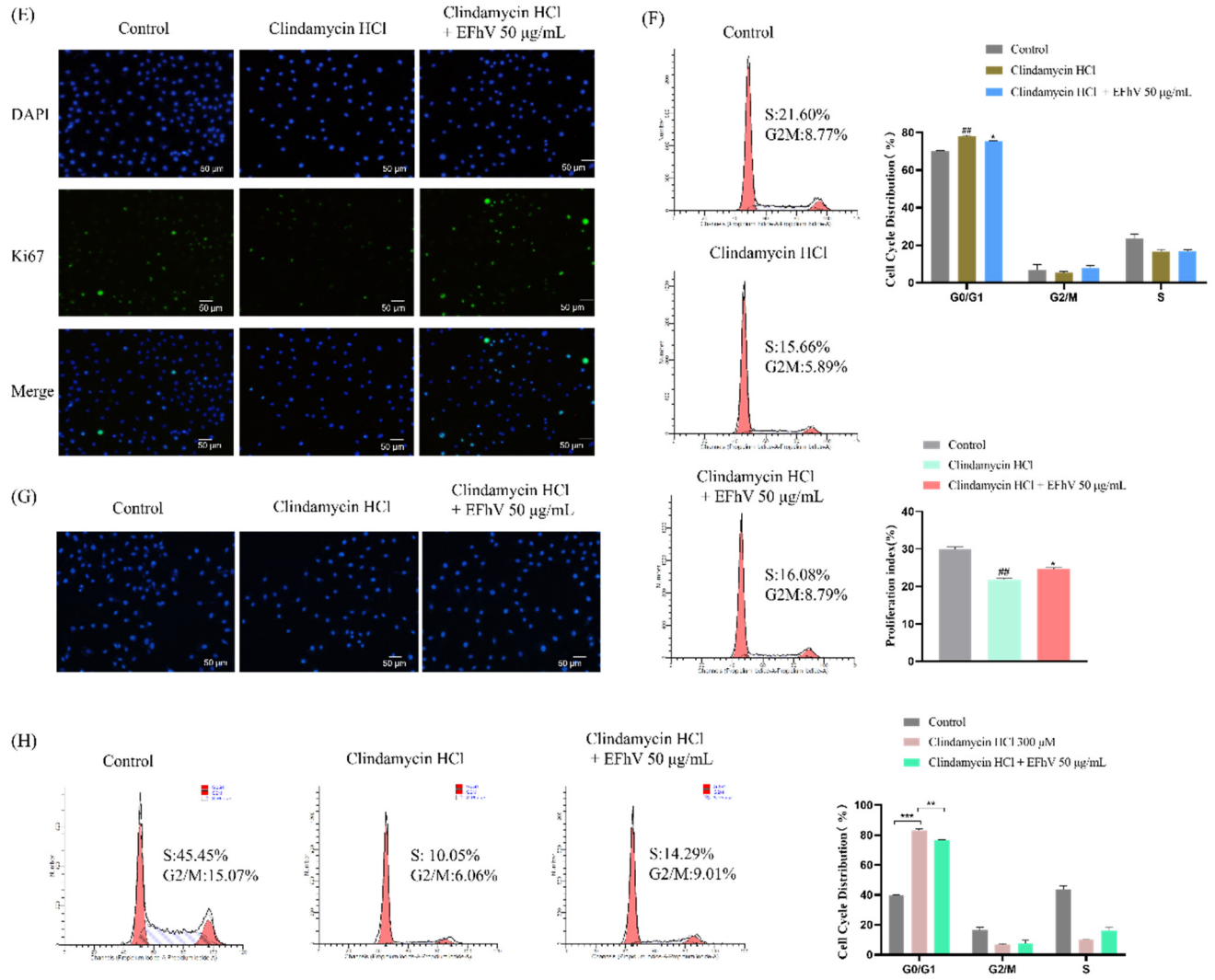

Figure 4. Effect of EFhV on IEC-6 cell and HCoEpiC cell antibiotic (Clindamycin HCl, 300 μmol/L) model. (A-B) Clindamycin HCl (300 μmol/L) and EFhV at different concentrations treated IEC-6 and HCoEpiC cells for cell viability. (C-D) Effects of Clindamycin HCl and EFhV 50 μg/mL on IEC-6 and HCoEpiC cells migration. (E) The effect of Clindamycin HCl and EFhV 50 μg/mL on Ki67 in IEC-6 cells was determined by immunofluorescence. (F) The cell cycle of IEC-6 cells treated with Clindamycin HCl and EFhV at 50 μg/mL was determined by flow cytometry. (G) Hoechst 33258 detected the effect of Clindamycin HCl and EFhV 50 μg/mL on IEC-6 cell apoptosis. (H) The effect of antibiotic and EFhV 50 μg/mL on the cell cycle of HCoEpiC cells. Values are means ± SEM, n = 3. $^{\#}P < 0.05$, $^{\#\#}P < 0.01$, $^{\#\#\#}P < 0.001$ compared with control group and $^{*}P < 0.05$, $^{**}P < 0.01$, $^{***}P < 0.001$ compared with antibiotic group.

In conclusion, EFhV acted on the intestinal epithelial injury model induced by antibiotic, and the results showed that EFhV could alleviate the G0/G1 phase arrest in the cell cycle caused by Clindamycin HCl, reverse the abnormal expression of Ki67, and play a role in intestinal repair after injury.

3.4 EFhV targets microRNA-195/HNMT pathway in intestinal epithelial cells.

Studies have shown that overexpression of microRNA-195 disrupts intestinal epithelial homeostasis. Here, we explored whether the EFhV promotes intestinal epithelial cell proliferation and repair by post-transcriptionally regulating microRNA-195 expression. PCR results showed that EFhV (50 μg/mL) significantly downregulated miR-195 expression in IEC-6 cells (Figure 5A). Transfection with microRNA-195 mimics increased miR-195 expression, reducing cell viability and inhibiting IEC-6 cell growth (Figures 5B-5D).

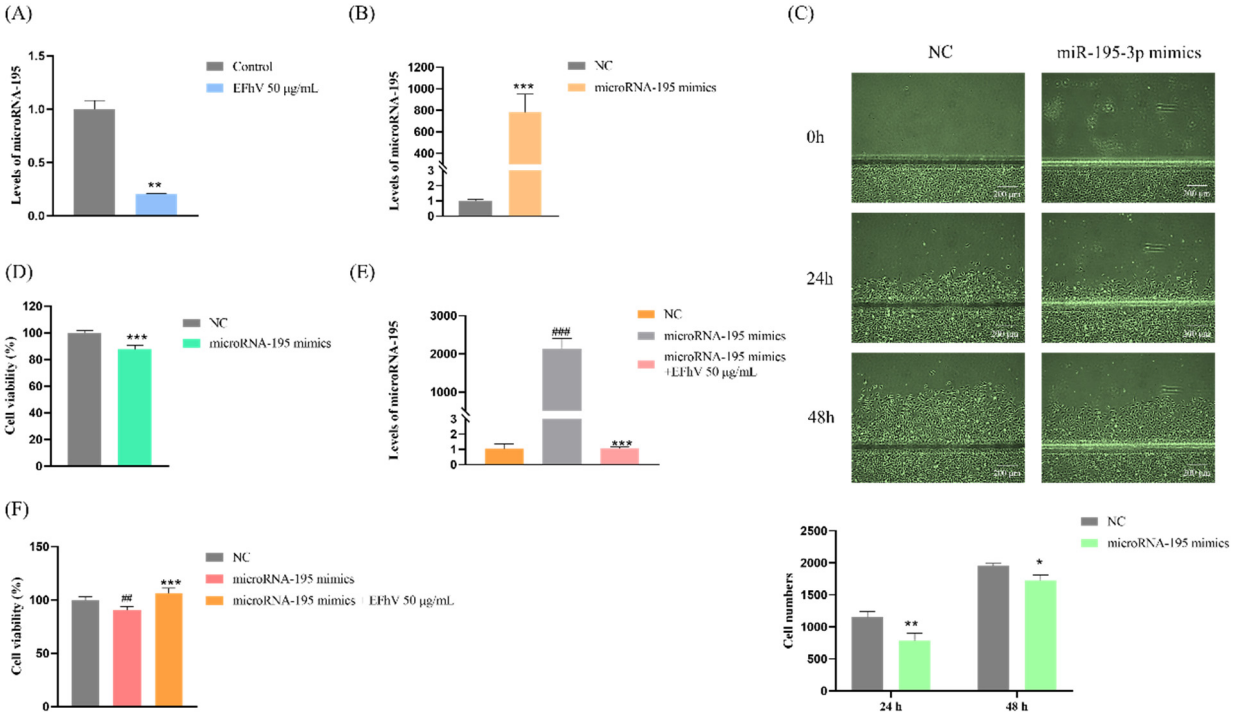
(A)
Levels of microRNA-195
Control
EFhV 50 μg/mL
**
(B)
Levels of microRNA-195
NC
microRNA-195 mimics
***
(C)
NC
miR-195-3p mimics
0h
24h
48h
(D)
Cell viability (%)
NC
microRNA-195 mimics
***
(E)
Levels of microRNA-195
NC
microRNA-195 mimics
microRNA-195 mimics +EFhV 50 μg/mL
###
***
(F)
Cell viability (%)
NC
microRNA-195 mimics
microRNA-195 mimics + EFhV 50 μg/mL
##
***
Cell numbers
NC
microRNA-195 mimics
**
*
24 h
48 h

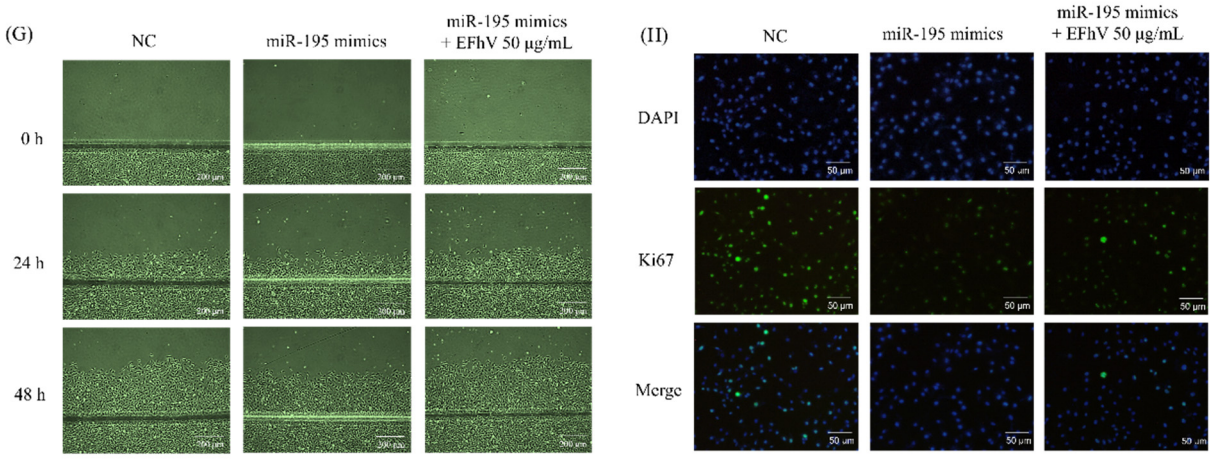
(G)
NC
miR-195 mimics
miR-195 mimics + EFhV 50 μg/mL
0 h
24 h
48 h
(II)
NC
miR-195 mimics
miR-195 mimics + EFhV 50 μg/mL
DAPI
Ki67
Merge
50 μm

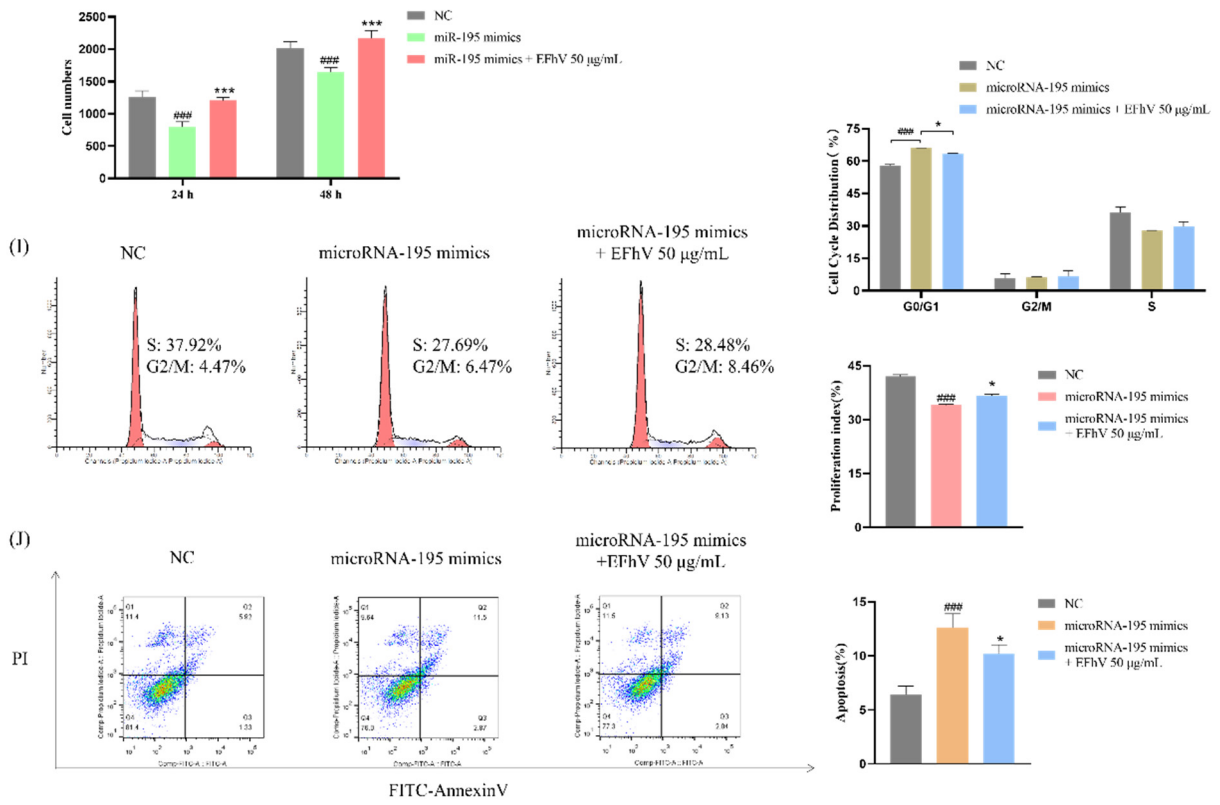

Figure 5. Effect of EFhV on microRNA-195 expression in IEC-6 cells and its effects on cellular functions following microRNA-195 overexpression. (A) Effect of EFhV (50 μg/mL) on microRNA-195 expression in IEC-6 cells. (B) RT-qPCR result demonstrated the transfection effect of microRNA-195 mimics. (C) Inhibition of IEC-6 cell proliferation after overexpression of microRNA-195. (D) Inhibition of IEC-6 cell migration after overexpression of microRNA-195. Values are means ± SEM, n = 3. $^{*}P < 0.05$, $^{**}P < 0.01$, $^{***}P < 0.001$ compared with the control group. (E) The effect of EFhV 50 μg/mL on the expression level of microRNA-195 after microRNA-195 overexpression. (F) Effect of EFhV 50 μg/mL on cell viability after overexpression of microRNA-195 in IEC-6 cells. (G) Effect of EFhV 50 μg/mL on IEC-6 cell migration after overexpression of microRNA-195. (H) The effect of EFhV 50 μg/mL on Ki67 in IEC-6 cells after overexpression of microRNA-195 was detected by immunofluorescence. (I) The cell cycle of IEC-6 cells treated with EFhV 50 μg/mL after microRNA-195 overexpression was detected. (J) Apoptosis of IEC-6 cells treated with EFhV 50 μg/mL after microRNA-195 overexpression was detected. Values are means ± SEM, n = 3. $^{###}P < 0.001$ compared with the NC group and $^{*}P < 0.05$, $^{***}P < 0.001$ compared with the microRNA-195 mimics group.

Next, after the overexpression of miR-195, co-treatment of EFhV for 48h could reverse the decreased cell viability caused by the overexpression of miR-195 (Figures 5E-5F). The wound-healing assay showed that the overexpression of miR-195 combined with the EFhV could enhance the restitution after wounding of IEC-6 cells (Figure 5G). Furthermore, immunofluorescence analysis showed that EFhV rescued reduction of Ki67 in IEC-6 cells caused by the overexpression of miRNA-195 (Figures 5H). Flow cytometry results indicated that EFhV could alter the distribution in the G0/G1 phase and reverse the growth inhibition of IEC-6 cells caused by overexpression of miR-195 (Figure 5I). And it suppressed the overexpression of miR-195-induced IEC-6 cell apoptosis (Figure 5J).

Using bioinformatics prediction tools TargetScan and miRDB, along with literature-reported filtered proteins involved in intestinal epithelial function, we identified differences in the expression of histamine *N*-methyltransferase (HNMT) transcripts between inflammatory bowel disease (IBD) patients and the control group. HNMT serves as an indicator reflecting the functional integrity of the intestinal mucosa (Figure 6A)[24,25], however, to date, no studies have explored its potential role in protecting the intestinal

epithelium. Western blot method was used to detect the expression level of the biomarker HNMT in IEC-6 cells, which was induced by the overexpression of miR-195. The results revealed co-treatment with EFhV reversed the reduced expression of HNMT caused by the overexpression of miR-195 (Figure 6B). Furthermore, PCR experiments indicated that the level of HNMT mRNA also decreased after the overexpression of miR-195, but recovered after co-treatment with EFhV (Figure 6C). These data indicated that the EFhV protects the intestinal epithelium by reversing the downregulation of HNMT caused by microRNA-195 overexpression for the first time.

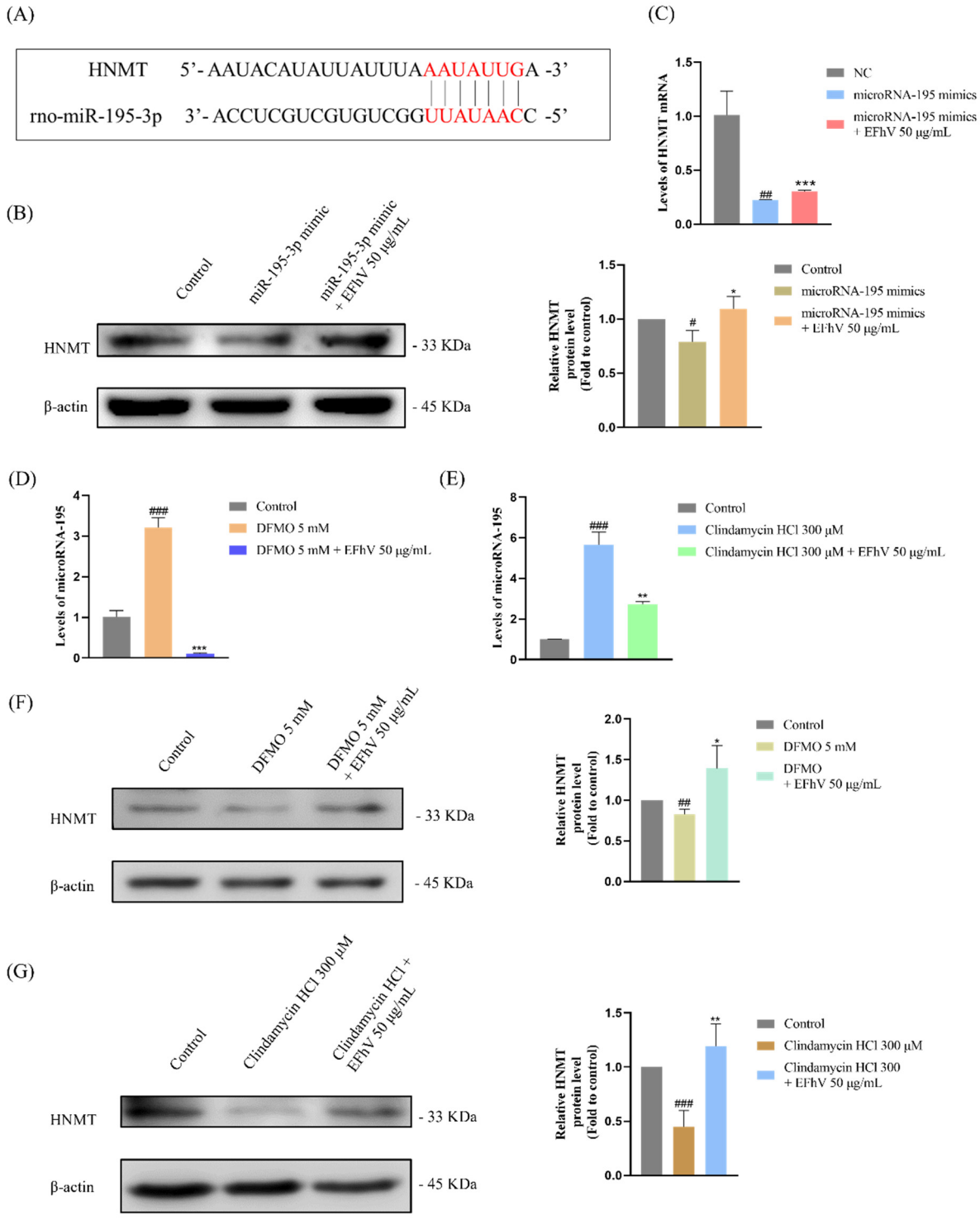

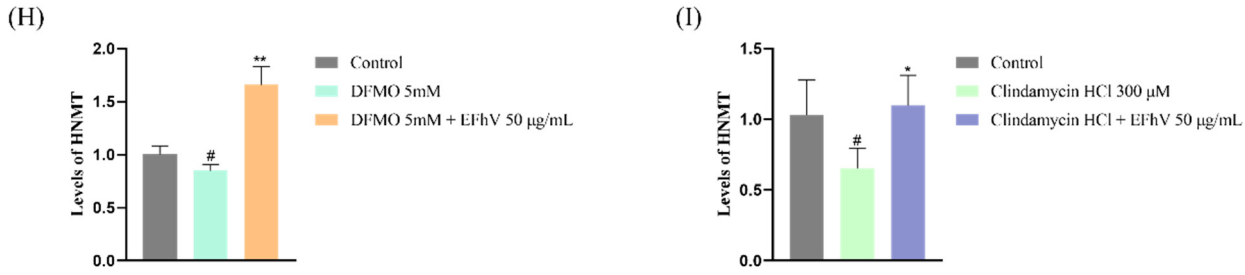

Figure 6. Effect of EFhV (50 μg/mL) on microRNA-195 and HNMT protein. (A) Sequence alignment results of MicroRNA-195 and HNMT. (B) Western Blot results showed the effect of EFhV 50 μg/mL on HNMT protein expression after overexpression of microRNA-195. (C) RT-qPCR results showed the effect of EFhV 50 μg/mL on HNMT mRNA after overexpression of microRNA-195. Values are means ± SEM, n = 3. $^{\#}P < 0.05$, $^{\#\#}P < 0.01$ compared with the NC group and $*P < 0.05$, $***P < 0.001$ compared with the microRNA-195 mimics group. (D) The changes of microRNA-195 levels in IEC-6 cell DFMO (5 mmol/L) model after EFhV (50 μg/mL) treatment. (E) The changes of microRNA-195 levels after EFhV were treated with 50 μg/mL Clindamycin HCl (300 μmol/L) in IEC-6 cell antibiotic model. (F) Western Blot assay showed the effect of EFhV (50 μg/mL) in DFMO (5 mmol/L) model on HNMT protein expression. (G) Protein western blotting assay showed the effect of EFhV 50 μg/mL in Clindamycin HCl (300 μmol/L) model on HNMT protein expression. (H-I) RT-qPCR results showed the changes of HNMT mRNA in IEC-6 cell DFMO model and antibiotic model treated with EFhV (50 μg/mL). Values are means ± SEM, n = 3. $^{\#}P < 0.05$, $^{\#\#}P < 0.01$, $^{\#\#\#}P < 0.001$ compared with the control group, $*P < 0.05$, $**P < 0.01$, $***P < 0.001$ compared with the DFMO and antibiotic group.

3.5 The regulative impact of EFhV on microRNA-195 and HNMT in damaged intestinal cell models.

The above study found that the reversing effect of EFhV on the growth inhibition of IEC-6 cells in the intestinal epithelial injury model induced by DFMO and antibiotics, which might be related to the expression of microRNA-195. To further validate this concept, we conducted RT-qPCR experiments to examine the changes in microRNA-195 expression levels in both the DFMO and antibiotic models, as well as the influence of co-treatment with EFhV on microRNA-195 expression in these models. The results revealed that microRNA-195 expression was significantly upregulated in the DFMO-treated IEC-6 cells and in the clindamycin HCl-induced antibiotic model. However, co-treatment with EFhV for 48 hours effectively reversed the overexpression of microRNA-195 (Figures 6D-6E). Additionally, our findings indicated that the protein expression and mRNA levels of HNMT were downregulated in the DFMO and antibiotic-treated groups, whereas these levels were restored upon co-treatment with EFhV (Figures 6F-6I). These results suggest that EFhV can mitigate the overexpression of microRNA-195 in the DFMO and antibiotic models, thereby reversing the effects of DFMO and antibiotics on HNMT protein and mRNA expression. Collectively, these findings indicate that the upregulation of miR-195 in DFMO and antibiotic-induced intestinal epithelial injury may represent one of the mechanisms underlying the growth inhibition of IEC-6 cells. Furthermore, EFhV appears to protect intestinal epithelial cells in DFMO and antibiotic models via modulation of the miR-195/HNMT axis.

When intestinal injury or inflammation arises, the tightly regulated mucosal homeostasis is disrupted, potentially compromising the integrity of the intestinal barrier. Under stress conditions, intestinal epithelial cells must rapidly receive signals and respond appropriately to regulate epithelial cell survival and maintain mucosal homeostasis. Fasting and starvation can result in inadequate nutrient intake, leading to intestinal dysbiosis, increased intestinal permeability, and the induction of intestinal inflammation, all of which contribute to impaired intestinal barrier function[9,29]. Consequently, we employed a rat model of intestinal

mucosal injury induced by fasting/starvation and treatment with the antibiotic (clindamycin HCl) to investigate the protective effects of the EFhV on the rat intestine. Furthermore, considering the current scarcity of universally accepted drugs for intestinal mucosal recovery and miR-195-3p regulation, we selected glycyrrhetinic acid (GA) as a positive drug, which was previously reported to exhibit intestinal protective effect[23].

3.6 EFhV promotes the recovery of intestine barrier injury in fasting rat models through microRNA-195/HNMT

The *in vivo* protective effect of EFhV on intestine barrier injury in fasting (FAST) model rats was evaluated (Figure 7A). Compared to the FAST group, the rate of weight loss in rats decreased after administration of EFhV (250 mg/kg and 750 mg/kg) and GA (25 mg/kg) (Figure 7B), suggesting the ability to slow down the weight loss of rats after administration may be related to the repair of intestinal. The H&E staining results revealed fasting-induced intestinal damage (Figures 7C-7D), the FAST group exhibited shortened intestinal villi, irregular mucosal arrangements, and reduced crypt numbers compared to the controls. Both EFhV and GA effectively attenuated small intestinal mucosal atrophy. In colonic tissues, fasting caused glandular disorganization, goblet cell depletion, and lamina propria inflammation. Notably, EFhV (750 mg/kg) demonstrated superior efficacy in mitigating colonic mucosal damage, achieving comparable effects to the positive drug GA. The immunohistochemical results (Figures 7E-7F) shown that the expression of HNMT protein in the small intestine and colon of rats in the FAST group decreased, and both EFhV and GA could significantly reverse the expression of HNMT. Furthermore, the PCR analysis results revealed that the expression of miR-195 was significantly upregulated in the small intestine and colon tissues of rats in the FAST model group, and EFhV and GA administration rescued miR-195 expression level (Figures 7G-7H). These results illustrated that EFhV could protect facilitate the repair of intestinal and colonic mucosal injury in fasting rats by modulating miR-195-HNMT.

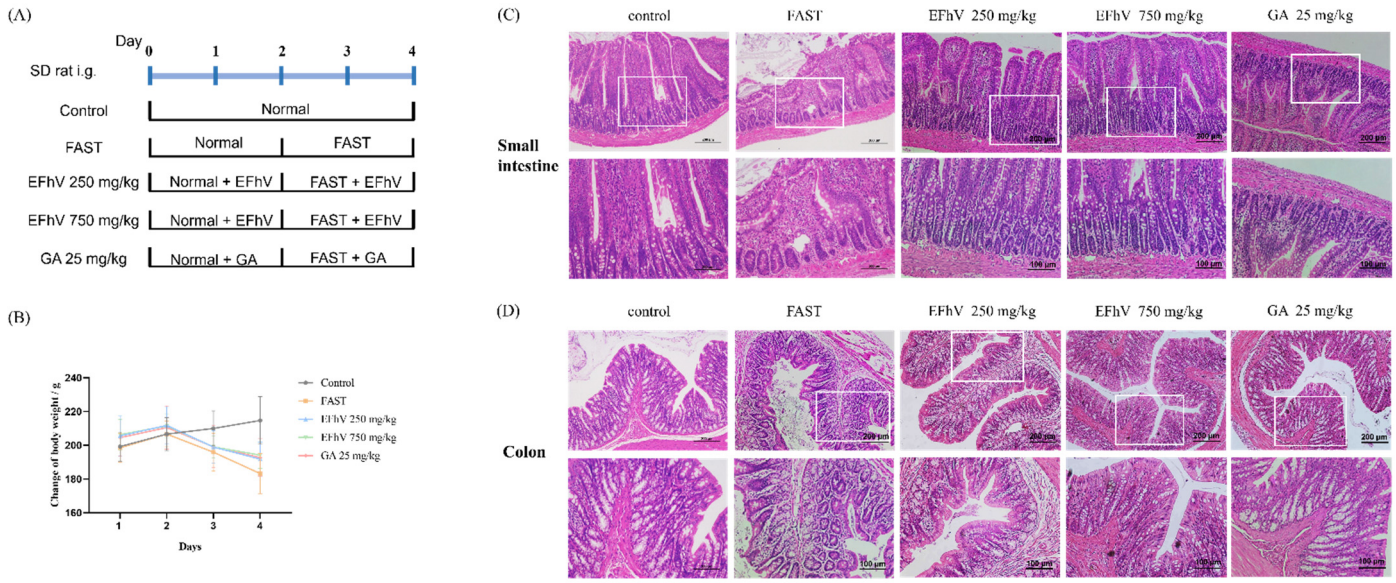

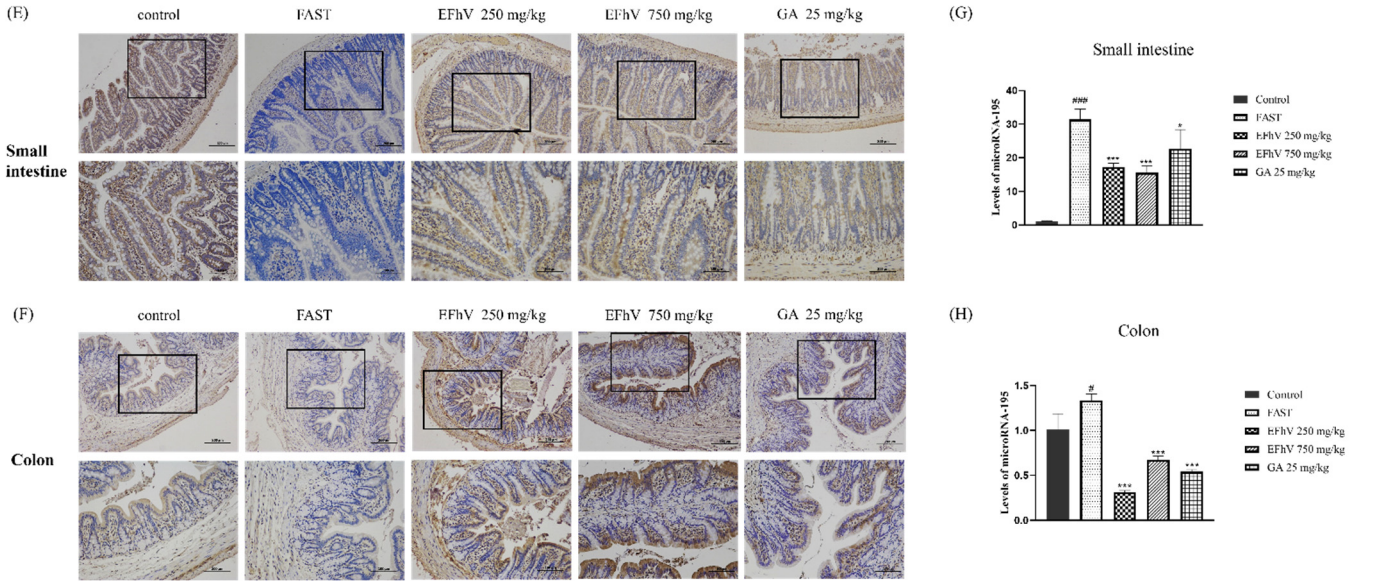

Figure 7. The *in vivo* protective effect of EFhV (250 mg/kg, 750 mg/kg, i.g.) on intestine barrier injury in fasting (FAST) rat model. (A) Experimental procedure of the FAST model. (B) Body weight changes in the FAST model rats. (C-D) Morphological changes of small intestine and colon tissues of rats in FAST model groups (H&E staining, 100× and 200×). (E-F) Small intestine and colon tissues in rats. (G-H) Levels of microR-195 in small intestine and colon tissues treated with FAST and EFhV as measured by Q-PCR. Values are means ± SEM, n = 3. $^{\#}P < 0.05$, $^{\#\#\#}P < 0.001$ compared with control group, $^{*}P < 0.05$, $^{***}P < 0.001$ compared with antibiotic group.

3.7 EFhV promotes the recovery of intestine barrier injury in antibiotic-induced rats through microRNA-195/HNMT

The *in vivo* protective effect of EFhV on intestine barrier injury antibiotic-induced rats was also evaluated, and the experimental process was shown in Figure 8A. Notably, we observed that antibiotic treatment did not significantly affect the weights of the rats (Figure 8B). The H&E staining revealed significant intestinal pathology (Figures 8C-8D), presenting shortened intestinal villi, crypt atrophy and structural distortion, as well as inflammatory infiltration of the mucosal layer. While both EFhV and GA partially ameliorated these mucosal injuries, with EFhV (750 mg/kg) demonstrating best therapeutic efficacy. The immunohistochemical analysis further supported that antibiotic administration for 7 days significantly reduced HNMT protein expression in intestinal and colonic tissues, which was reversed by EFhV and GA treatments (Figures 8E-8F). Then, the PCR analysis results also revealed that the elevated miR-195 levels in intestinal tissues of antibiotic-treated rats were substantially normalized following EFhV or GA intervention (Figures 8G-8H). These results illustrated that EFhV could protect facilitate the repair of intestinal and colonic mucosal injury antibiotic-induced rats by modulating miR-195-HNMT. *In vivo* studies have shown that EFhV can improve intestinal epithelial damage caused by fasting and antibiotic models, as well as reverse the abnormal expression of HNMT and microRNA-195 in these models.

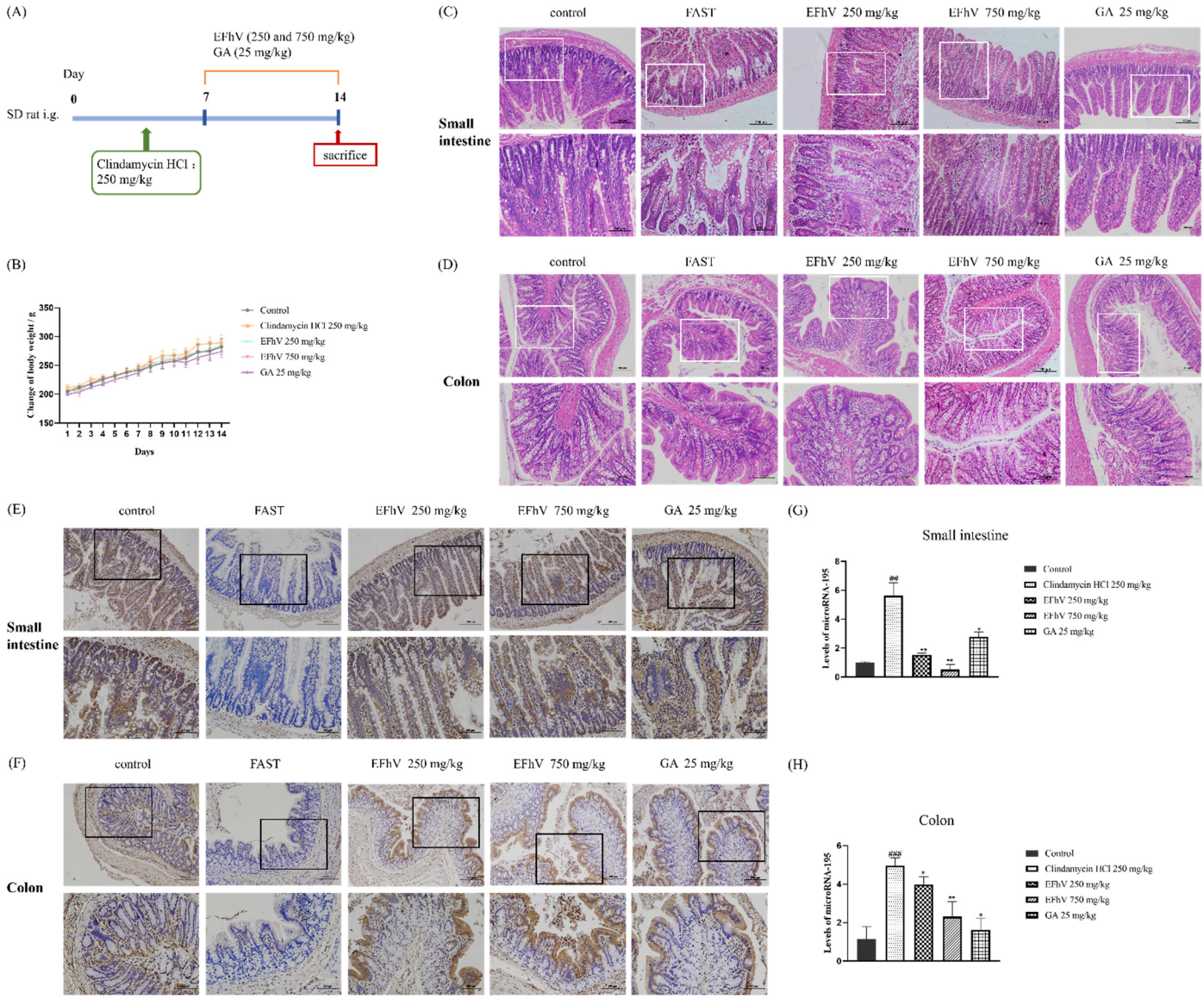

Figure 8. The *in vivo* protective effect of EFhV (250 mg/kg, 750 mg/kg, i.g.) on intestine barrier injury in antibiotic rat model. (A) Experimental procedure of the antibiotic model. (B) Body weight changes in the antibiotic model rats. (C-D) Morphological changes of small intestine and colon tissues of rats in antibiotic model groups (H&E staining, 100× and 200×). (E-F) Small intestine and colon tissues in rats. (G-H) Levels of microR-195 in small intestine and colon tissues treated with Clindamycin HCl and EFhV as measured by Q-PCR. Values are means ± SEM, n = 3. $^{\#}P < 0.05$, $^{\#\#}P < 0.01$, $^{\#\#\#}P < 0.001$ compared with control group, $^{*}P < 0.05$, $^{**}P < 0.01$ compared with antibiotic group.

4. Discussion

This study provides the first evidence that *Ficus hirta* Vahl. ethanol extract (EFhV) exerts protective effects on intestinal epithelium through post-transcriptional regulation of the microRNA-195/HNMT pathway *in vitro* and *in vivo*. Our findings demonstrate that EFhV promotes proliferation and repair of intestinal epithelial cells (IEC-6) andcolonic epithelial cells (HCoEpiC) under both physiological and pathological conditions. Notably, EFhV alleviated growth inhibition and apoptosis induced by DFMO and antibiotics in IECs, likely by suppressing microRNA-195 overexpression and restoring HNMT protein expression. The discovery of microRNA-195 as a negative regulator of HNMT, and its modulation by EFhV, offers novel mechanistic insights into the intestinal protective effects of this traditional medicinal plant.

The association between microRNA-195 and intestinal epithelial integrity has been previously suggested[30], but no studies have linked its regulation to natural product-mediated protection. Our work bridges this gap by identifying HNMT, a protein linked to mucosal integrity, as a direct target of microRNA-195 in IECs. The EFhV-mediated downregulation of microRNA-195 and subsequent HNMT restoration highlights a unique post-transcriptional mechanism underlying its therapeutic potential. These findings align with traditional applications of *F. hirta* in gastrointestinal health and expand its pharmacological relevance to modern nutraceutical development.

Interestingly, our results also resonate with the "lung-gut axis" theory in traditional medicine. While this study focused on intestinal protection, *F. hirta*'s documented anti-inflammatory effects on lung tissues suggest potential cross-organ protective mechanisms[31]. Studies have demonstrated that the primary bioactive constituents of *F. hirta* include flavonoids and phenylpropanoids, such as psoralen, bergapten, and apigenin[32], which exhibit anti-inflammatory and antioxidant properties and may confer benefits to pulmonary or intestinal health[33-35]. Further investigation into its bioactive component and their dual roles in pulmonary and intestinal health could unveil broader therapeutic applications.

5. Conclusions

In conclusion, this study establishes EFhV as a promising candidate for mitigating intestinal epithelial damage through the microRNA-195/HNMT axis. However, future work should isolate the specific active constituents of EFhV and validate its efficacy in clinical models of gut barrier dysfunction. These findings not only advance the functional food potential of *F. hirta* but also provide a mechanistic framework for developing miRNA-targeted interventions in gastrointestinal disorders.

Acknowledgments

This work was financially supported by National Key R&D Program of China (2024YFC3506400), National Natural Science Foundation of China (82404479), The Open Project of Key Laboratory of High Altitude Medicine (Ministry of Education) (2025-KF-02, Central and provincial financial funds for Qinghai University), Joint Plan of Liaoning Province Science and Technology Program (2024-MSLH-435, 2024-MSLH-420), excellent youth support program of Shenyang pharmaceutical university (YQ202205). China Postdoctoral Science Foundation (2024MD753957), Postdoctoral Fellowship Program of CPSF (GZC20231733).

Conflict of interest

The authors declare no conflict of interest. The funders had no role in the design of the study; in the collection, analyses, or interpretation of data; in the writing of the manuscript, or in the decision to publish the results.

References

[1] M. Fu, Q.W. Wang, Y.R. Liu, S.J. Chen, The role of the three major intestinal barriers in ulcerative colitis in the elderly, Ageing Res Rev 108 (2025) 102752. https://doi.org/10.1016/j.arr.2025.102752.

[2] L.W. Peterson, D. Artis, Intestinal epithelial cells: regulators of barrier function and immune homeostasis, Nat Rev Immunol 14 (3) (2014) 141-153. https://doi.org/10.1038/nri3608.

[3] R. Okumura, K. Takeda, Roles of intestinal epithelial cells in the maintenance of gut homeostasis, Exp Mol Med 49 (5) (2017) e338. https://doi.org/10.1038/emm.2017.20.

[4] M.A. Odenwald, J.R. Turner, The intestinal epithelial barrier: a therapeutic target? Nat Rev Gastroenterol Hepatol 14 (1) (2017) 9-21. https://doi.org/10.1038/nrgastro.2016.169.

[5] D.C. Shi, P.Y. Wang, L. Xu, et al., Potential of *Dendrobium officinale* oligosaccharides to alleviate chronic colitis by modulating inflammation and gut microbiota. Food & Medicine Homology, 2025, 2 (2025) 9420077. https://doi.org/10.26599/FMH.2025.9420077.

[6] S.S. Zhang, D. Feng, J.Z. An, et al. Total Glycosides of *Cistanche deserticola* attenuates DSS-induced inflammatory bowel disease by regulating intestinal environmental homeostasis. Food & Medicine Homology, 2 (2025) 9420048. https://doi.org/10.26599/FMH.2025.9420 048.

[7] H. Duan, L.L. Yu, F.W. Tian, et al., Antibiotic-induced gut dysbiosis and barrier disruption and the potential protective strategies, Crit Rev Food Sci Nutr 62 (6), (2022) 1427-1452. https://doi.org/10.1080/10408398.2020.1843396.

[8] S. Becattini, Y. Taur, E.G. Pamer, Antibiotic-induced changes in the intestinal microbiota and disease, Trends Mol Med 22 (6) (2016) 458-478. https://doi.org/10.1016/j.molmed.2016.04.003.

[9] S. Attia, M. Feenstra, N. Swain, et al., Starved guts: Morphologic and functional intestinal changes in malnutrition, J Pediatr Gastroenterol Nutr 65 (5) (2017) 491-495. https://doi.org/10.1097/MPG.0000000000001629.

[10] D. Zhou, Z.S. Bai, T.T. Guo, et al., Dietary flavonoids and human top-ranked diseases: The perspective of *in vivo* bioactivity and bioavailability, Trends Food Sci. Tech. 120 (2022) 374-386. https://doi.org/10.1016/j.tifs.2022.01.019.

[11] P.Y. Wang, M. Cai, K. Yang, et al., Phenolics from *Dendrobium officinale* leaf ameliorate dextran sulfate sodium-induced chronic colitis by regulating gut microbiota and intestinal barrier, J Agric Food Chem71 (44) (2023) 16630-16646. https://doi.org/10.1021/acs.jafc.3c05339.

[12] Y.M. Liu, C. Liu, Y.S. Deng, et al. Beneficial effects of dietary herbs on high-fat diet-induced obesity linking with modulation of gut microbiota. Food & Medicine Homology, 2 (2025) 9420034. https://doi.org/10.26599/FMH.2025.9420 034.

[13] R.M. Xiao, G.J. Luo, W.C. Liao, et al., Association of human gut microbiota composition and metabolic functions with *Ficus hirta* Vahl dietary supplementation, NPJ Sci. Food. 6 (1) (2022) 45. https://doi.org/10.1038/s41538-022-00161-3.

[14] X.S. Ye, W.J. Tian, G.H. Wang, et al., Phenolic glycosides from the roots of *Ficus hirta* Vahl. and their antineuroinflammatory activities. *J. Agric. Food Chem*. **2020**, *68* (14), 4196-4204. https://doi.org/10.1021/acs.jafc.9b07876.

[15] X.S. Ye, W.J. Tian, G.H. Wang, et al., Four undescribed coumarin derivatives, with ten amides from the roots of *Ficus hirta* and their cytotoxic activities, Bioorg Chem 144 (2024) 107116. https://doi.org/10.1016/j.bioorg.2024.107116.

[16] R.M. Xiao, G.J. Luo, S.L. Liang, et al., Functional polysaccharide from *Ficus hirta* Vahl: Digestive properties, anti-inflammation, and effect on gut microbiota *in vitro*, ACS Food Sci Technol 4 (3) (2024) 719-729. https://doi.org/10.1021/acsfoodscitech.3c00626.

[17] M. Insanu, F.R.C. Santoso, I. Fidrianny, A review of the phytochemical compounds and pharmacological activities from selected *Ficus* plants, Int J Pharm Sci Res 11 (Suppl.4) (2020) 921-928. https://doi.org/10.26452/ijrps.v11iSPL4.4225.

[18] B. Salehi, A. Prakash Mishra, M. Nigam, et al., *Ficus* plants: State of the art from a phytochemical, pharmacological, and toxicological perspective, Phytother Res 35 (3) (2021**)** 1187-1217. https://doi.org/10.1002/ptr.6884.

[19] J.R. Finnerty, W.X. Wang, S.S. Hébert, et al., The miR-15/107 group of microRNA genes: evolutionary biology, cellular functions, and roles in human diseases, J Mol Biol 402 (3) (2010) 491-509. https://doi.org/10.1016/j.jmb.2010.07.051.

[20] X.Y. Yang, J. Yu, J. Yin, et al., MiR-195 regulates cell apoptosis of human hepatocellular carcinoma cells by targeting LATS2, Pharmazie 67 (7) (2012) 645-651.

[21] S.R. Wang, N. Rathor, M.S. Kwon, et al., MiR-195 regulates intestinal epithelial restitution after wounding by altering actin-related protein-2 translation, Am J Physiol Cell Physiol 322 (4) (2022) C712-C722. https://doi.org/10.1152/ajpcell.00001.2022.

[22] S.Z. Hu, H.T. Zhou, X.K. Zhao, et al., MiR-195-5p suppresses gastric adenocarcinoma cell progression via targeting OTX1, Histol Histopathol 38 (6) (2023) 659-668. https://doi.org/10.14670/HH-18-512.

[23] Y.J. Wang, D. Zhou, X.N. Zhang, et al., Curcumin promotes renewal of intestinal epithelium by miR-195-3p, J Ethnopharmacol 320 (2024) 117413. https://doi.org/10.1016/j.jep.2023.117413.

[24] H.A. Schulze, R. Häsler, N. Mah, et al., From model cell line to *in vivo* gene expression: disease-related intestinal gene expression in IBD, Genes Immun 9 (3) (2008) 240-248. https://doi.org/10.1038/gene.2008.11.

[25] M. Camilleri, P. Carlson, N. Valentin, et al., Pilot study of small bowel mucosal gene expression in patients with irritable bowel syndrome with diarrhea, Am J Physiol Gastrointest Liver Physiol *311* (3) (2016) G365-G376. https://doi.org/0.1152/ajpgi.00037.2016.

[26] X.N. Zhang, X.Y. Wen, D. Zhou, et al., Lycibarbarspermidine L from the fruit of *Lycium barbarum* L. recovers intestinal barrier damage via regulating miR-195-3p, J Ethnopharmacol 320 (2024) 117419. https://doi.org/10.1016/j.jep.2023.117419.

[27] H. Yoon, M. Schaubeck, I. Lagkouvardos, et al., Increased pancreatic protease activity in response to antibiotics impairs gut barrier and triggers colitis, Cell Mol Gastroenterol Hepatol 6 (3) (2018) 370-388. https://doi.org/10.1016/j.jcmgh.2018.05.008.

[28] Y. Feng, Y.W. Li, D. Zhou, et al., Glycyrrhetinic acid reverses antibiotic-induced intestinal epithelial injury through RNA-binding protein human antigen R (HuR), Phytomedicine 94 (2022) 153836. https://doi.org/10.1016/j.phymed.2021.153836.

[29] J.Y. Mao, Y.H. Yan, H.L. Li, et al., Glutamine deficiency links clindamycin-induced dysbiosis and intestinal barrier dysfunction in mice, Br J Nutr 126 (3) (2021) 366-374. https://doi.org/10.1017/S0007114520004195.

[30] Y.J. Wang, X.N. Zhang, M.L. Qing, W. Dang, X.M. Bai, Y.J. Wang, D. Zhou, L.J. Zhu, D.G. Qing, J. Zhang, G. Chen, N. Li. Trends in intestinal aging: From underlying mechanisms to therapeutic strategies, Acta Pharmaceutica Sinica B 15 (7) (2025) 3372-3403. https://doi.org/10.1016/j.apsb.2025.05.011.

[31] M. Chen, J. Liu, S. Zou, et al., A review on the ethnopharmacology, metabolites, pharmacological uses, and toxicology of *Ficus hirta* (Moraceae) Vahl, Front Pharmacol 16 (2025) 1545348. https://doi.org/10.3389/fphar.2025.1545348.

[32] J. Zeng, H. Yu, Integrated metabolomic and transcriptomic analyses to understand the effects of hydrogen water on the roots of *Ficus hirta* Vahl. Plants (Basel). 11(5) (2022) 602. https://doi.org/10.3390/plants11050602.

[33] Y.X. Wang, J. Zhang, S.H. Xu, et al., Psoralen alleviates acute lung injury by covalently targeting Cys106 of HMGB1 in macrophages to inhibit inflammatory responses, Phytomedicine 142 (2025) 156807. https://doi.org/10.1016/j.phymed.2025.156807.

[34] T. Luo, X. Jia, W.D. Feng, et al., Bergapten inhibits NLRP3 inflammasome activation and pyroptosis via promoting mitophagy, Acta Pharmacol Sin 44 (9) (2023) 1867-1878. https://doi.org/10.1038/s41401-023-01094-7.

[35] S.Q. Cai, Z.M. Tang, C. Xiong, et al., The anti-inflammatory effects of apigenin and genistein on the rat intestinal epithelial (IEC-6) cells with TNF-α stimulation in response to heat treatment, Curr Res Food Sci 5 (2022) 918-926. https://doi.org/10.1016/j.crfs.2022.05.011